

Phase diagram for the Ashkin-Teller model in three dimensions

Ruth V. Ditzian and Jayanth R. Banavar
*The James Franck Institute, University of Chicago,
 5640 South Ellis Avenue, Chicago, Illinois 60637*

G. S. Grest
Physics Department, Purdue University, West Lafayette, Indiana 47907

Leo P. Kadanoff
*The James Franck Institute, University of Chicago,
 5640 South Ellis Avenue, Chicago, Illinois 60637*

(Received 12 December 1979)

High- and low-temperature series, Monte Carlo simulations, mean-field calculations, and renormalization-group ideas are used to analyze the behavior of the Ashkin-Teller model in three dimensions. The data generated by series and Monte Carlo methods in the neighborhood of the decoupling point are consistent with the renormalization-group conclusion that this system cannot show a line of continuously varying exponents. Thus the phase diagram for the $d=3$ system is quite different from that in $d=2$. Indeed a new phase (not seen in $d=2$) is observed, one in which the system spontaneously breaks its natural symmetry between its two kinds of Ising spins. A variety of continuous transitions are observed and explained in terms of an analysis which is fully consonant with renormalization-group concepts.

I. INTRODUCTION

The Ashkin-Teller (AT) model¹ may be considered to be two superposed Ising models, which, respectively, are described by variables σ_i and S_i sitting on each of the sites of a hypercubic lattice. Within each Ising model, there is a two-spin nearest-neighbor interaction with strength J_2 . In addition, the different Ising models are coupled by a four-spin interaction with strength J_4 . Thus the Hamiltonian is

$$H = - \sum_{\langle ij \rangle} [J_2(\sigma_i \sigma_j + S_i S_j) + J_4 \sigma_i \sigma_j S_i S_j] \quad , \quad (1.1)$$

where the sum covers all nearest neighbors on a lattice.

This model has a rich structure in two dimensions. Our knowledge of the two-dimensional structure has been obtained from series analysis,^{2,3} exact duality statements^{4,5} (including connections with the 8-vertex model solved by Baxter⁶), by expansions about the point ($J_4=0$) at which the model reduces to two decoupled Ising models, and by quasiexact analysis of limiting cases.⁷ Unfortunately, much less data can be obtained in three dimensions. Neither the duality statements nor the connections with the 8-vertex model apply to the three-dimensional case. The expansion about the decoupling point also gives much weaker information in three dimensions than in two. For $d=2$, J_4 is seen to be a marginal field, i.e., one which is capable of generating a line of critical points. In general J_4 has a scaling index at the

decoupling point which is given by

$$y_4 = 2/\nu - d \quad . \quad (1.2)$$

For three dimensions^{8,9} $\nu \sim 0.64$, and so y_4 turns out to be greater than zero. This says that J_4 is a relevant field, i.e., one which is capable of completely changing the nature of the critical point. Thus, in three dimensions, there might be three completely different critical behaviors for small $x = J_4/J_2$ depending upon whether x is just less than zero, just greater than zero, or exactly equal to zero. This possible structure at the decoupling point is a first indication that the Ashkin-Teller model might have a phase diagram in three dimensions which is quite different from the known $d=2$ form.

In fact this complex structure was indicated by the ϵ -expansions of models with symmetries analogous to that of the Ashkin-Teller model.¹⁰⁻¹² This type of analysis showed three different types of behavior as the possible end points of flows arising near the decoupling point. One flow is to a fixed point which describe two decoupled Ising models, another leads to no stable fixed point and hence indicates a first-order phase transition, and the third is to a $n=2$ critical point analogous to that of the XY or planar model. Hence, we should not be surprised if our analysis shows these three behaviors for $x=0$, $x \geq 0$, and $x \leq 0$.

An earlier series study² of the AT model in three dimensions seemed to show that the critical index γ varied continuously with x near $x=0$. This conclu-

sion, if valid, would imply that there was a serious error in the predictions of the renormalization group. One of the major reasons for undertaking the research described here was to see whether the behavior of this system could be explained by assuming the correctness of the renormalization-group conclusions.

The present work seeks to establish the nature of the phase diagram for the three-dimensional Ashkin-Teller model by using several complementary techniques.¹³ Our results are obtained by using data from high- and low-temperature series for the free energy, magnetizations, and susceptibilities and the importance-sampling Monte Carlo technique. These results, when used in conjunction with exact statements for limiting cases and with hints obtained from mean-field theory, lead to a rich phase diagram with several multicritical points.

We find that the series analysis method and Monte Carlo technique, while each having their own strengths and weaknesses, effectively complement each other. While it is possible to determine the critical exponents and the transition temperature accurately using series analysis in simpler parts of the phase diagram (where crossover effects are not dominant), the Monte Carlo technique is useful in finding the different types of ordering and the transition temperatures even in complicated regions of the phase diagram. Even then (as discussed in Sec. IV), our results are not entirely without ambiguities.

In the next section, we introduce our problem by summarizing the known information about the two-dimensional problem. Section III is devoted to a description of the mean-field-theory calculation. Then, the main body of our work is presented in Sec. IV, which describes the most relevant series data and the results of the Monte Carlo analysis. The technique for obtaining and analyzing the series and a brief description of the Monte Carlo method are described in the Appendixes.

II. THE TWO-DIMENSIONAL CASE

Figure 1 gives the phase diagram^{3,5,7} of the Ashkin-Teller model on a two-dimensional square lattice plotted as a function of $x = J_4/J_2$ and a coupling strength, $J_2/kT = K_2$. Let us list the phases shown.

(a) Paramagnetic, labeled as "para." If the couplings are sufficiently weak the system falls into a paramagnetic phase in which neither σ nor S (nor anything else) is ordered.

(b) A "Baxter" phase in which σ and S independently order in a ferromagnetic fashion so that $\langle \sigma \rangle = \pm \langle S \rangle$. It is also true that $\langle S\sigma \rangle$ is unequal to zero and has the same sign as $\langle S \rangle \langle \sigma \rangle$. This phase appears when the condition $x \geq -1$ is satisfied and

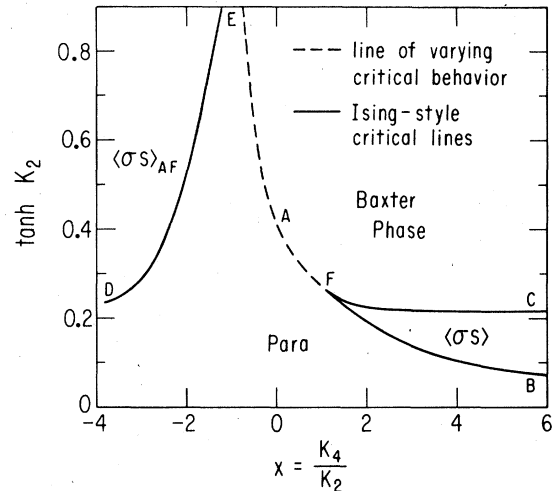


FIG. 1. Phase diagram of the Ashkin-Teller model in two dimensions. The exact positions of the Ising style critical lines are not known.

the temperature is sufficiently low (or the couplings are sufficiently strong).

(c) A phase labeled $\langle \sigma S \rangle$, in which σS is ordered ferromagnetically but $\langle \sigma \rangle = \langle S \rangle = 0$. This phase arises for large K_4 (which then tends to order σS) and small J_2 (which permits σ and S to remain individually disordered).

(d) An analogous antiferromagnetic phase (labeled $\langle \sigma S \rangle_{AF}$) which arises for large negative J_4 and small J_2 . In this phase σ and S are individually disordered but their product, σS , is ordered antiferromagnetically.

A fuller understanding of this phase diagram may be obtained by focusing upon the points labeled A, B, C, The point A is a decoupling point at which the AT model decomposes into two independent Ising models. As mentioned above, in two dimensions (only) this is a point at which a marginal operator may be shown to appear and to generate a line isomorphic¹⁴ to the known critical line of the 8-vertex model. In Fig. 1, this line of continuously varying second-order phase transitions goes from E to A to F. Its exact position is known via a duality statement and the variation of critical indices from ($\alpha = -1$ at E) to ($\alpha = 0$ at A) to ($\alpha = \frac{2}{3}$ at F) is probably also known exactly.

Near points B and D, K_2 becomes negligibly small and the entire ordering is produced by

$$K_4 = K_2 x \quad .$$

In the neighborhood of these points, the AT model simply reduces to an Ising model in the variable σS . In any dimensionality, the condition for criticality at B and D reduces to

$$K_4 = \pm K_c^I \quad , \quad (2.1)$$

where K_c^l is the critical coupling for the Ising model in the appropriate dimensionality. The transition near points B and D may be analyzed by doing second-order perturbation theory in the small quantity K_2 . The result is that the second-order Ising transition persists in these neighborhoods and the curves of criticality for x are

$$x = \pm K_c^l / K_2 - K_2 . \quad (2.2)$$

Near point C , K_4 is very large. Hence σS is ordered fully and ferromagnetically. Consider for example, the particular phase in which $\langle \sigma S \rangle = 1$. Then with a very high probability, S_i will take on a value equal to σ_i . In the neighborhood of the point C then, the system will be governed by an effective Hamiltonian in the variable $\sigma_i = S_i$, which Hamiltonian has the form

$$H = -2J_2 \sum_{\langle ij \rangle} \sigma_i \sigma_j + J_4 \sum_{\langle ij \rangle} 1 . \quad (2.3)$$

This Hamiltonian will then produce a second-order Ising-style phase transition for

$$K_2 = \frac{1}{2} K_c^l$$

in the neighborhood of point C . This result may also be expected to hold for higher dimensions. In fact, one can estimate the order of magnitude of the corrections to this result by looking at the probability for producing a situation in which σS is misaligned at one point in a d -dimensional hypercubic lattice. The result is that for large x

$$K_2 = \frac{1}{2} K_c^l + O(e^{-2dxK_c^l}) . \quad (2.4)$$

The point F lies at $x = 1$. At this value of x , the AT model has the additional symmetry of the four-state Potts model for which the replacements

$$\sigma_i \rightarrow \sigma_i S_i ; \quad S_i \rightarrow S_i , \quad (2.5)$$

are a symmetry operation additional to the usual Ashkin-Teller symmetry operation

$$\sigma_i \rightarrow S_i , \quad S_i \rightarrow \sigma_i . \quad (2.6)$$

In two dimensions (but not three) the four-state Potts model is known to have a second-order phase transition. Moreover the point F is known to be a bifurcation point at which the line EF splits into two transition lines as shown in Fig. 1. The exact form of the curves FC and FB (which are believed to be second-order Ising lines along their entire length for $d = 2$) is not known.

The AT model also shows a special symmetry on the line $x = -1$. For this case, the Hamiltonian takes the form

$$H = -J_2 \sum_{\langle ij \rangle} (\sigma_i \sigma_j + S_i S_j - \sigma_i S_i \sigma_j S_j) .$$

To see the symmetry divide the system into two sublattices A and B such that each A site has as its nearest neighbors B sites. Of course this division is possible on a square lattice or a hypercubic one. Then, on the B sublattice flip the signs of the spins, making the replacement

$$\sigma_i \rightarrow -\sigma_i , \quad S_i \rightarrow -S_i , \quad (2.7)$$

on B sublattice the Hamiltonian now becomes

$$H = J_2 \sum_{\langle ij \rangle} (\sigma_i \sigma_j + S_i S_j + \sigma_i \sigma_j S_i S_j) . \quad (2.8)$$

For positive J_2 this Hamiltonian cannot induce any long-range order in two dimensions, and will, in fact, produce a paramagnetic state for all $J_2 > 0$, as can be seen from the Baxter solution of the 8-vertex model. Thus the entire line $x = 1$, including the lowest nonzero temperatures, is paramagnetic in two dimensions. As $K_2 \rightarrow \infty$, the width in x of the paramagnetic region shrinks to zero so that the "Baxter" and $\langle \sigma S \rangle_{AF}$ phases approach the $x = -1$ line.

Apart from this point at $x = -1$, the system falls into simple ground states at zero temperature. If $x > -1$, the ground state has σ , S , and σS ordered ferromagnetically. If $x < -1$, the ground state has σS ordered antiferromagnetically but σ and S disordered. Energetic analysis also shows that these ground states are also formed in higher dimensionalities in exactly these regions, $x \gtrless -1$.

To complete the phase diagram of Fig. 1, one must draw a phase boundary between the paramagnetic phase and the antiferromagnetic one. The exact form and nature of this boundary is not known, except near point D , but it is reasonable to assume that it connects the points E and D as shown and that it has the character of a second-order Ising antiferromagnetic transition throughout.

III. MEAN-FIELD THEORY

It is often said that mean-field theory represents in some sense the infinite dimensional limit of statistical systems.¹⁵ If this is true, it is particularly interesting for us to study the mean-field behavior of the AT model so that we may effectively bracket the three-dimensional system between the mean field and the $d = 2$ behaviors.

To write the mean-field equations, let $j(i)$ represent the set of all nearest neighbors to the site i . Then the potentials acting upon the spins σ , S , and σS at the site i are, respectively, h_σ^i , h_S^i , and $h_{\sigma S}^i$ where

$$\begin{aligned} h_\sigma^i &= \sum_{j(i)} \langle \sigma_{j(i)} \rangle K_2 , \\ h_S^i &= \sum_{j(i)} \langle S_{j(i)} \rangle K_2 , \\ h_{\sigma S}^i &= \sum_{j(i)} \langle \sigma_{j(i)} S_{j(i)} \rangle K_4 . \end{aligned} \quad (3.1)$$

The spins at site i feel the effective Hamiltonian

$$H_{\text{eff}}^i = h_{\sigma}^i \sigma_i + h_S^i S_i + h_{\sigma S}^i \sigma_i S_i . \quad (3.2)$$

The single-site partition function generated by the Hamiltonian (3.2) is

$$Z^i = 4 (\cosh h_{\sigma}^i \cosh h_S^i \cosh h_{\sigma S}^i + \sinh h_{\sigma}^i \sinh h_S^i \sinh h_{\sigma S}^i) . \quad (3.3)$$

This Hamiltonian may also be used to calculate the average of the spins at the site i in the form¹⁶:

$$\begin{aligned} \langle \sigma_i \rangle &= (\tanh h_{\sigma}^i + \tanh h_S^i \tanh h_{\sigma S}^i) / D , \\ \langle S_i \rangle &= (\tanh h_S^i + \tanh h_{\sigma}^i \tanh h_{\sigma S}^i) / D , \\ \langle \sigma_i S_i \rangle &= (\tanh h_{\sigma S}^i + \tanh h_{\sigma}^i \tanh h_S^i) / D , \\ D &= 1 + \tanh h_{\sigma}^i \tanh h_S^i \tanh h_{\sigma S}^i . \end{aligned} \quad (3.4)$$

As is usual in mean-field calculations, one can also obtain the basic averages by demanding that an approximate free-energy function

$$\begin{aligned} F = - \sum_i \ln Z^i + K_2 \sum_{\langle ij \rangle} (\langle \sigma_i \rangle \langle \sigma_j \rangle + \langle S_i \rangle \langle S_j \rangle) \\ + K_4 \sum_{\langle ij \rangle} \langle \sigma_i S_i \rangle \langle \sigma_j S_j \rangle \end{aligned} \quad (3.5)$$

be minimized by the correct choice of the averages. The minimization conditions obtained by substituting Eq. (3.3) into Eq. (3.5) and then differentiating with respect to the averages is, in fact, just the set of mean-field Eqs. (3.4). Thus we shall solve these equations. Whenever we obtain several solutions, we pick the solution which minimizes the free energy given by Eqs. (3.5).

The mean-field equations can then be used to explore the possible behaviors of a whole variety of possible phases of the system. Figure 2 describes the result of studying the relative stability of all the phases mentioned above. For example, to study the $\langle \sigma S \rangle_{\text{AF}}$ phase, we set $\langle \sigma \rangle = \langle S \rangle = 0$ everywhere and let $\langle \sigma_i S_i \rangle$ alternate in signs upon the two sublattices. Since this particular phase apparently remains stable up to the line $x = -1$, we are impelled also to study the phase which is its counterpart under the symmetry operations appropriate for the Hamiltonian (2.8). This phase has σ ordered ferromagnetically but $\langle S \rangle$ and $\langle \sigma_i S_i \rangle$ vanishing. There is also an equivalent phase with $\langle S \rangle \neq 0$, but $\langle \sigma \rangle = \langle \sigma S \rangle = 0$. At the line $x = -1$, the system apparently undergoes a first-order phase transition from the phase $\langle \sigma S \rangle_{\text{AF}}$ into this new phase, which we denote by $\langle \sigma \rangle$.

The mean-field-theory phase diagram as shown in Fig. 2 does give a suggestive picture of what behavior might be expected for $d=3$. As expected there are lines of second-order phase transitions emerging from the points B , C , and D . In the mean-field calculation, at the point A' , to the right of the decou-

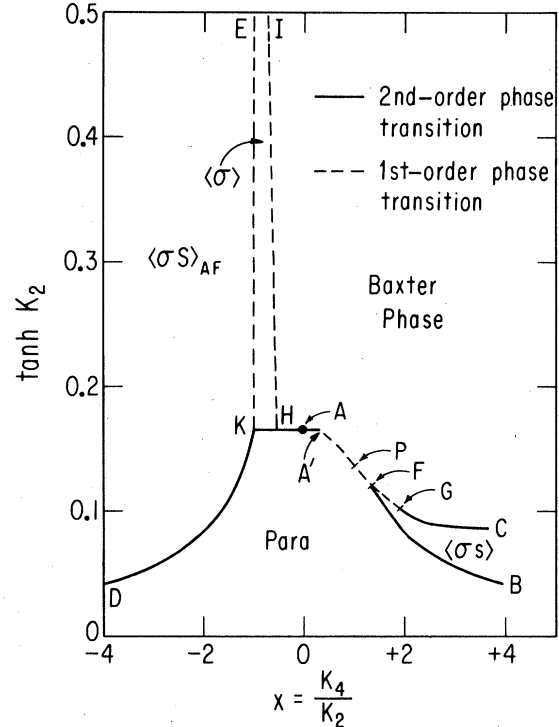


FIG. 2. Mean-field theory phase diagram for the Ashkin-Teller model.

pling point A , the transition between the paramagnetic and the "Baxter" phase becomes first order. This first-order transition persists through the point P , which lies on the Potts line, until the point F at which the line of phase transition bifurcates into two. The lower line, FB represents a second-order phase transition between the paramagnetic and the $\langle \sigma S \rangle$ phase. The upper line FGC separates the $\langle \sigma S \rangle$ and Baxter phases. It is a first-order transition in the region FG and becomes second order thereafter.

To the left of the decoupling point there is a second-order phase transition along the line AH which separates the Baxter and paramagnetic phases. Then at $x = -\frac{1}{2}$, a new phase $\langle \sigma \rangle$ appears. This phase is squeezed between two first-order lines which come together at $x = -1$. The line separating the $\langle \sigma \rangle$ and $\langle \sigma S \rangle_{\text{AF}}$ phases, KE , lies exactly at $x = -1$. Finally, the $\langle \sigma S \rangle_{\text{AF}}$ and paramagnetic phases are separated by a second-order line, KD . Our mean-field analysis does not indicate the existence of a phase with $\langle \sigma \rangle$ and $\langle S \rangle$ being unequal and different from zero. This contradicts the results of our Monte Carlo analysis (Sec. IV), which seems to indicate the possibility of such an ordering in three dimensions.

Notice that mean-field theory indicates a somewhat different low-temperature ($K_2 \rightarrow \infty$) behavior than that seen in two dimensions. In $d=2$, for large K_2 , as x increases through the value -1 , the system suc-

cessively passes through the phases $\langle \sigma S \rangle_{AF}$, para, and "Baxter." As K_2 gets larger and larger these phases get closer and closer to one another. The mean-field picture is the same, except that the intermediate phase is not paramagnetic as in $d = 2$, but " $\langle \sigma \rangle$."

IV. APPLICATION OF SERIES DATA AND MONTE CARLO ANALYSIS

Figure 3 shows our proposed phase diagram for the three-dimensional AT model and indicates some of the data we have used to support the assignment of this diagram. Recall that we know quite precisely the behavior of the system in the neighborhoods of the

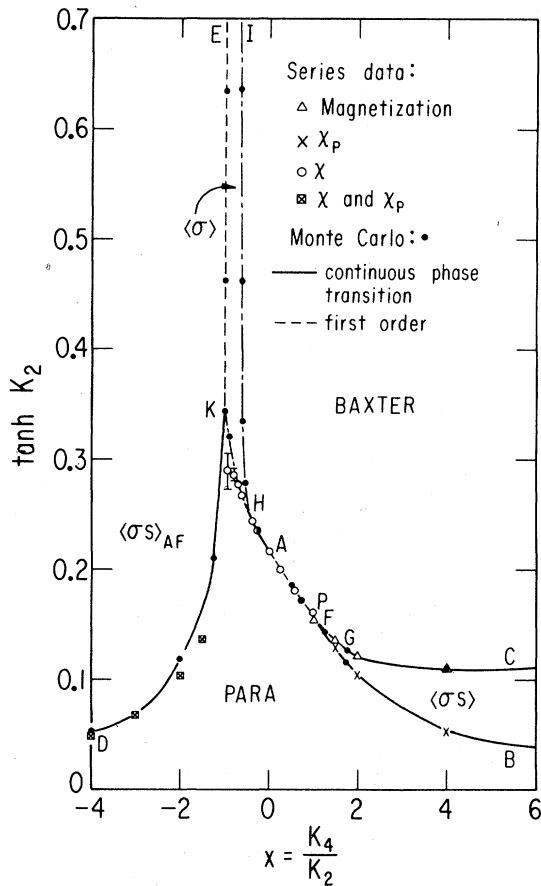


FIG. 3. Phase diagram of the Ashkin-Teller model in three dimensions obtained from series analysis and Monte Carlo simulations. The nature of the transition HI has not been established unambiguously (see Sec. IV for a discussion). The phase transition FB is believed to show an Ising critical structure as does GC and KD . AFG is believed to be first order while AH is a continuous transition with XY exponents. The behavior on KH is unknown. Error bars are shown on a few series points. For those without an error bar, the apparent error is smaller than the size of the plotted point.

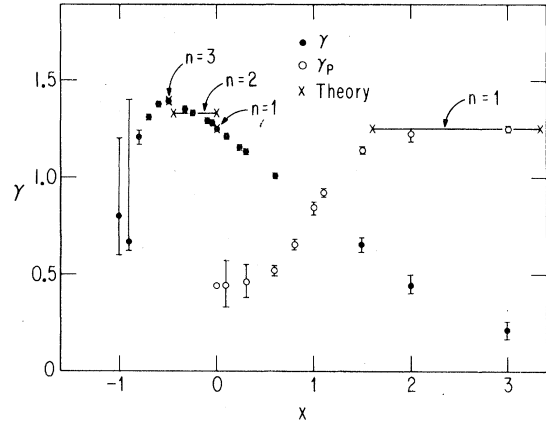


FIG. 4. Plot of series estimates of γ and γ_p as a function of x . "Theory" shows accepted γ values as a function of n plotted where we believe they might apply.

points B , C , and D . That is, we know that there is a second-order phase transition in these neighborhoods which are characteristic of an Ising ferro- or antiferromagnetic transition, and we know the nature of the states on both sides of the transition. Furthermore, we know that point A has the character of two decoupled Ising transitions and that there is a relevant operator which can make the transitions just to the left and to the right of point A to have totally different character from each other and from that at A . The series analysis and the Monte Carlo technique effectively complement each other in filling in the rest of the phase diagram.

A first indication of the behavior near A is given by an analysis of the magnetic susceptibility. We obtained a 10-term high-temperature series (see Appendix B) in the usual magnetic susceptibility

$$\chi = \sum_{JK} \langle \sigma_J \sigma_K \rangle \tag{4.1a}$$

and for the corresponding quantity constructed from σS , i.e.,

$$\chi_p = \sum_{JK} \langle \sigma_J S_J \sigma_K S_K \rangle \tag{4.1b}$$

We call the latter quantity the polarization susceptibility. To analyze the series, we fixed $x = J_4/J_2$ and obtained expansions in $V = \tanh K_2$. Padé and ratio analyses of the singularities in these quantities show a reasonably well-converged singularity and enable us to calculate the related critical indices γ and γ_p as a function of x . Figure 4 is a plot of these critical index values. Some of the critical values of $\tanh K_2$ related to these series are plotted in Fig. 3.

A. The region $0 < x < 1$

Now focus upon the region between A and F in Fig. 3 and the corresponding region between $x = 0$

and 1 in Fig. 4. At $x=0$, there are only five nonzero terms in the series for χ_p , so we cannot gain much information from the value of γ_p near $x=0$. However γ seems to decrease continuously from 1.25 ± 0.01 at $x=0$ to 0.84 ± 0.03 at $x=1$. It would appear from these data (and from similar earlier data) that there exists a line of second-order transitions between A and P with continuously varying critical indices.

However, renormalization-group theory¹⁰⁻¹² suggests that such an explanation must be incorrect. There is no obvious marginal operator in the pair of three-dimensional Ising models which exist at point A . Hence we seek an alternative explanation. Mean-field theory suggests a first-order transition in this region. These values of γ might be a reflection of an approximate pseudospinodal behavior in a transition which is really first order.

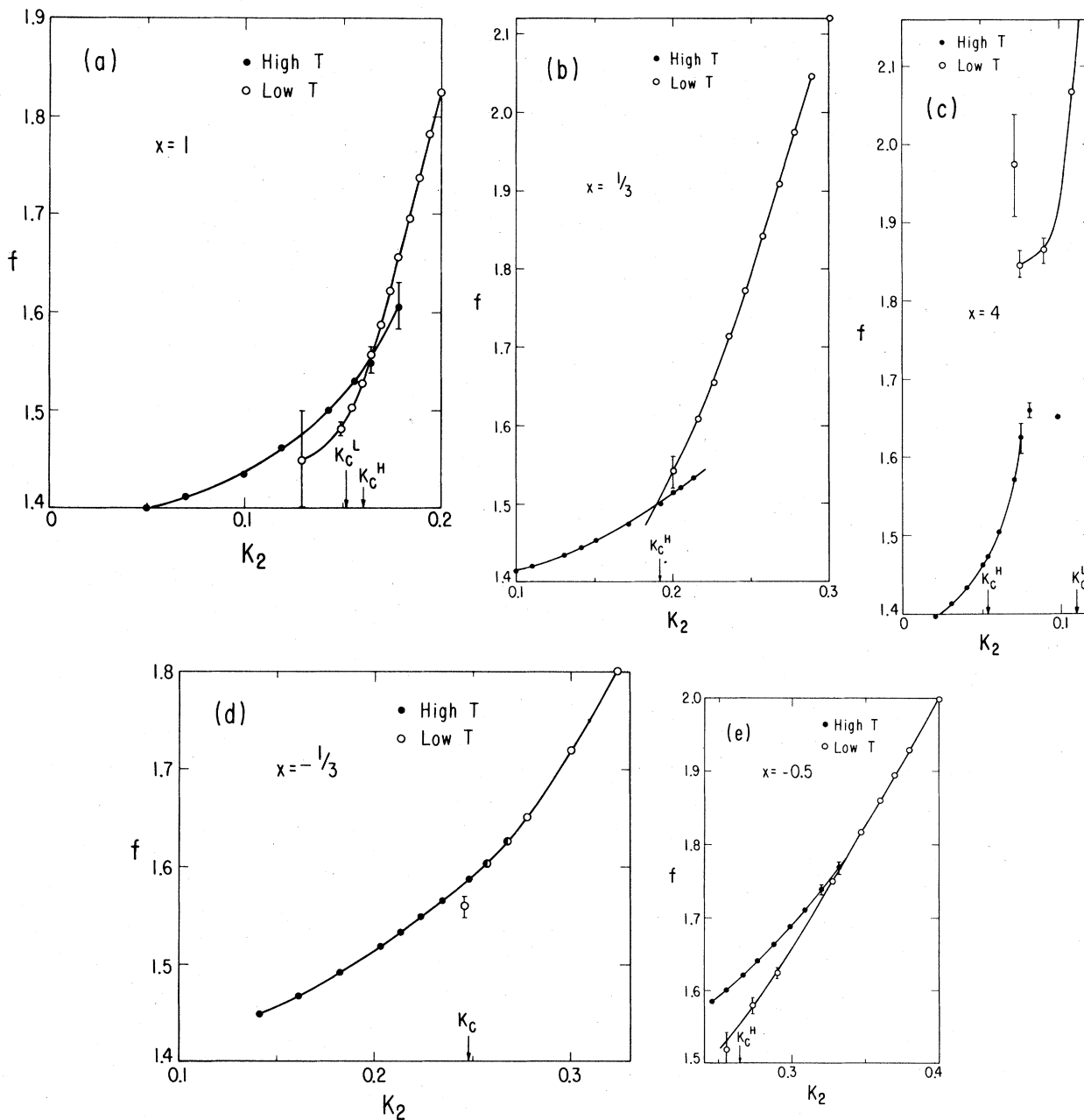


FIG. 5. Plots of the series estimates of the free energy f vs K_2 for various values of x . Error bars are shown, when the apparent errors exceed the size of the points. The critical values of K are K_c^H , taken from the high-temperature susceptibility series, and K_c^L , taken from the low-temperature magnetization series.

To examine this possibility, one needs low-temperature series for the free energy per site f , the magnetization

$$M = \left\langle \sum_i \sigma_i \right\rangle \quad (4.2a)$$

and the polarization

$$P = \left\langle \sum_i \sigma_i S_i \right\rangle. \quad (4.2b)$$

From past experience,^{17,18} we conclude that a comparison of T_c estimates from high- and low-temperature series do not provide the best way of distinguishing between first- and second-order phase transitions. The errors in T_c are sufficiently large to mask the effect under consideration. An alternative is to see where the high- and low-temperature series estimates of the free-energy f cross and then examine whether the crossing occurs with finite slope (a first-order transition) or zero slope (second order). The low temperature expansions were first obtained as double series in the variables $X = \exp[-4(K_2 + K_4)]$ and $Z = \exp(-4K_2)$. Convenient contact with the high-temperature analysis was made by fixing the ratio $x = K_4/K_2 = J_4/J_2$ so that the low-temperature variables were powers of one another, $X = Z^{1+x}$. When $1+x$ was chosen to be a simple rational fraction, series in a single low-temperature variable could be obtained and analyzed. For example, in the region we are now discussing, we analyzed low-temperature series for $x = \frac{1}{3}, \frac{1}{2},$ and 1. These series are respectively 48, 36, and 24 terms long and contain many zeros.

Figure 5 shows several plots of the reduced free energy per site,

$$f = -F/NKT. \quad (4.3)$$

Figure 5(a) shows a clear indication of free-energy crossing with nonzero difference in slope and hence a first-order transition for $x=1$. Figure 5(b) can be interpreted in several ways, but to our eyes it shows some indications of a first-order behavior at $x = \frac{1}{3}$. Hence, we tentatively identify the transition between $x=0$ and 1 as first order. Additional evidence for this identification can be found in the γ values in this region (see Fig. 4) which are lower than those in any of the standard three-dimensional universality classes. The apparent β values are also lower than the usual $d=3$ values, $\beta \approx \frac{1}{3}$, and are suggestive of a discontinuity—which could be represented by $\beta=0$. For example, $\beta = 0.17 \pm 0.05$ at $x = \frac{1}{3}$ and $\beta = 0.170 \pm 0.003$ at $x=1$. All in all, series data suggest a first-order behavior between $x=0$ and 1.

Monte Carlo data at $x=0.75$ also show clear evidence for a first-order transition, with discontinuous jumps in the magnetization and internal energy. For smaller x , the Monte Carlo analysis was less defini-

tive. At $x=0.5$, data were taken on a $10 \times 10 \times 10$ lattice. The transition temperature was unambiguously determined to be that indicated in the phase diagram (Fig. 3). The order parameter ($\langle \sigma \rangle$ or $\langle S \rangle$) and internal energy were plotted as a function of temperature. Reasonably smooth and continuous curves were obtained in both cases indicating that either the transition was continuous or if it was first order, it was only weakly so. The second possibility is not very surprising considering that $x=0.5$ is not too far from the tricritical point at $x=0$. Further data were taken with a $18 \times 18 \times 18$ lattice to clarify the nature of the transition. Starting from a random configuration, the system was quenched to a temperature slightly below the transition temperature and the internal energy was studied as a function of time. Some evidence could be seen for a relaxation process which occurs in two stages, being perhaps indicative of a system which has gotten "hung up" in a paramagnetic phase for up to a hundred and fifty Monte Carlo steps. These data partially support our inclination to believe in a first-order transition in the entire range between $x=0$ and 1.

B. The region $x \geq 2$

In this region, we can establish the position of the lower branch in Fig. 3 by looking for the divergence in the high-temperature series for the polarization susceptibility and the position of the upper branch by looking for zeros in the low-temperature magnetization. The latter calculation is performed at $x=8, 5, 4,$ and 2. The former calculation shows a clear value of $\gamma_p = 1.25$ for all $x \geq 2$ (see Fig. 4) so we interpret the lower branch once again as an Ising second-order transition in which $\langle \sigma S \rangle$ orders. For $x=4, 5,$ and 8 the upper branch appears as a zero in the magnetization series at one-half the critical coupling for the Ising transition; i.e., $K_2 = 0.110$, in accord with Eq. (2.4). At these points $\beta = 0.30 \pm 0.04$, so that the phase transition does appear to have an Ising character once more. At $x=2$, K_c has risen slightly, as suggested by Eq. (2.4) and we estimate β to be 0.24 ± 0.05 but the convergence of the series appears to be worse at $x=2$ than for larger x . One can interpret this decrease in β and worsened convergence to be indicative of an approach to tricritical behavior somewhere in the neighborhood of $x=2$. (Recall that, at a classical tricritical point, $\beta = \frac{1}{4}$.) For $x > 2$, our data therefore show a pair of Ising style second-order phase transitions just as in the mean-field theory or the two-dimensional case.

For $x=4$, the free-energy series [see Fig. 5(c)] supports this interpretation. The high- and low-temperature series never meet, so there must be a region (say between $K_2 = 0.54$ and 0.11) in which there is another phase entirely and neither free-energy

series correctly represents f . On the other hand, for $x = 2$, the free-energy data can be given any of several different interpretations so we cannot use these data in helping us decide whether the upper transition is first order or continuous.

Monte Carlo data were taken at $x = 4.0$. Two transitions (both continuous) were observed at temperatures (couplings) in excellent agreement with that obtained from series data. The transition at the lower temperature (higher coupling) was one in which σ and S became disordered, while σS remained ordered. The other transition was from this intermediate phase to a paramagnetic phase.

C. The region $1 < x < 2$

At $x = 1$, the Ashkin-Teller model reduces to a four-state Potts model which exhibits one first-order transition with finite latent heat.

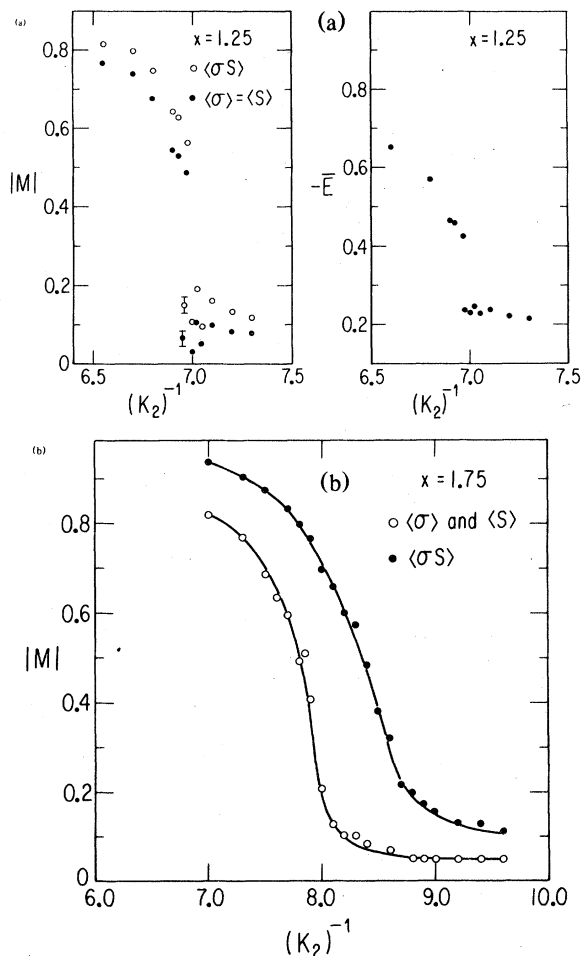


FIG. 6 (a) The absolute values of the magnetizations and internal energy as a function of the inverse coupling for $x = 1.25$. (b) The absolute values of the magnetizations as a function of the inverse coupling for $x = 1.75$.

At $x = 1.1$ and 1.25 , there was clear evidence from the Monte Carlo data for one and only one transition. Figure 6(a) shows a plot of the magnetization and internal energy as a function of temperature for $x = 1.25$. It is to be noted that σS , σ , and S all disorder at the same temperature. Discontinuous jumps in the magnetization and the internal energy confirm that the transition is first order. However, Monte Carlo data at $x = 1.50$ showed two transitions with the upper branch (higher coupling-lower temperature) being first order and the lower branch being continuous. This result is also indicated by the series data in which (at $x = 1.5$) the high-temperature estimate of K_c^{-1} (from χ_p) is significantly below the low-temperature estimate from the magnetization. Furthermore, the low value of $\beta(0.20 \pm 0.05)$ is again suggestive that the higher K_2 branch is first order. At $x = 1.75$, the Monte Carlo data suggest that there are two transitions, both transitions being continuous [see Fig. 6(b)].

The data at our disposal suggest the existence of a critical end point at $x = 1.4 \pm 0.1$ (where the splitting into two transitions takes place) (see point F in Fig. 3). The upper branch remains first order until a tricritical point at $x = 1.6 \pm 0.1$ is reached (see point G in Fig. 3). However, because it is difficult to distinguish between weakly first-order and second-order behavior and between two different phase transitions when they lie close to one another, the reader should be warned that our error estimates on the x values for the critical end point and the tricritical point are far from definitive.

D. The region $-0.5 < x < 0$

Our series analysis for small negative x indicates a continuous transition with indices suggesting possible XY behavior. The high-temperature susceptibility is well behaved until $x \sim -0.7$. The values of γ (Fig. 4) show a change from the Ising value of 1.25 through the XY value of 1.33 at $x = -0.25$ to the Heisenberg-like value of $\gamma = 1.39 \pm 0.01$ at $x = -0.5$. For $x < -0.5$, γ decreases while the singularity becomes less converged. The β value at $x = -\frac{1}{4}$ ($\beta = 0.305 \pm 0.040$) is also suggestive of a second-order behavior and consistent with the $n = 2$ value, $\beta = 0.33$. All this behavior is consistent with and suggestive of an XY -like transition in the region $0 > x > -0.5$ and a Heisenberg-like multicritical point at $x \sim -0.5$. The variation of the critical indices in the vicinity of the multicritical point may be attributed to crossover effects.¹⁹

The smooth meeting of free energies in Fig. 5(d) further indicates a continuous transition in the region $-0.5 < x < 0$. At $x = -\frac{1}{4}$ and $-\frac{1}{3}$, the critical point obtained from the low-temperature series is in good agreement with that obtained from the high-temperature series. At $x = -0.5$ [see Fig. 5(e)] the

free energies meet with equal slope but not at the location expected from the high-temperature analysis suggesting that we are in a complicated region. Monte Carlo data at $x = -0.25$ indicate a continuous transition from a ferromagnetically ordered state of σ and S to a paramagnetic state.

All these data, and the renormalization-group analysis as well, can be consistently interpreted by saying that for $-0.5 \leq x < 0$, the system has an $n = 2$ critical behavior.

E. The region $-4.0 \leq x < -0.5$

Monte Carlo data were taken at $x = -4.0$, -2.0 , and -1.25 . In all three cases clear evidence was found for one and only one continuous transition from a state where σS is ordered antiferromagnetically to a paramagnetic state. Figure 7 shows a plot of the order parameter as a function of the reduced temperature for $x = -2.0$ and -1.25 .

The series analysis is not very reliable to the left of $x = -0.5$. The complicated intermediate phase in the region $-0.5 > x > -1.0$ is very difficult to study using our series. For $x < -1.0$, we did not calculate series for the high-temperature staggered susceptibility, which would have been the best quantity to study in this region. On the other hand, the regular susceptibility is expected in an Ising transition to show a maximum near the antiferromagnetic transition. The critical-point data was therefore obtained by looking for a singularity in the logarithmic derivative of the susceptibility series. For large negative values of x , our series data are consistent with our Monte Carlo results and also with the analysis given in Eq. (2.1).

We remind the reader that the region $-1.0 \leq x$

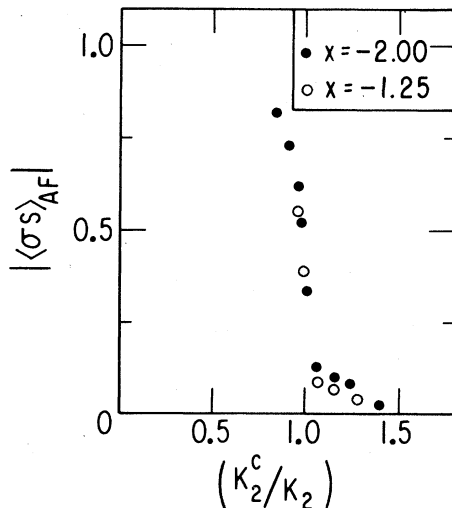


FIG. 7. The absolute value of the staggered magnetization $|\langle \sigma S \rangle_{AF}|$ plotted as a function of the reduced temperature for $x = -2.0$ and -1.25 .

< -0.5 is one in which mean-field theory predicts an intermediate phase at sufficiently low temperatures with the symmetry broken between the σ and S spins. To map the phase diagram, Monte Carlo runs were conducted both as a function of temperature for constant $x = K_4/K_2$ and as a function of x for constant K_2 .

The presence of the intermediate phase (labeled $\langle \sigma \rangle$ in the phase diagram, Fig. 3) was confirmed by studying the ordering as a function of x for $K_2 = 0.6$, 0.75 , and 1.5 . Figure 8 shows a plot of different magnetizations of a $10 \times 10 \times 10$ lattice versus x for $K_2 = 0.75$ and 1.5 . The figure clearly indicates a range of x values for which the ordering is such that $\langle \sigma \rangle \neq 0$ and $\langle S \rangle = \langle \sigma S \rangle = 0$.

The transition between the $\langle \sigma S \rangle_{AF}$ phase and the $\langle \sigma \rangle$ phase (the line KE in Fig. 3) occurs at $x = -1.0$ and is clearly first order since it is characterized by discontinuous jumps of the order parameters and a very small, possibly zero change in internal energy. Data taken at $x = -0.9$ as a function of K_2 suggest a continuous transition from the $\langle \sigma \rangle$ phase to the paramagnetic phase. From the Monte Carlo data, we estimate that the range of x values in which the $\langle \sigma \rangle$ phase exists shrinks to zero as $K_2 \rightarrow \infty$ or as $\tanh K_2 \rightarrow 1$.

To study the nature of the transition between the $\langle \sigma \rangle$ phase and the Baxter phase, Monte Carlo data were taken on a $14 \times 14 \times 14$ lattice at $K_2 = 0.75$ as a function of x . Over most of the range of x we see evidence for one of the two expected phases. For $-1 < x \leq -0.78$, there is a " $\langle \sigma \rangle$ " phase in which one of the pair $\bar{\sigma} = (1/N) \sum_j \sigma_j$ or $\bar{S} = (1/N) \sum_j S_j$ is negligibly small and the other has a value of order unity. For $-0.75 \leq x$ the Monte Carlo system falls

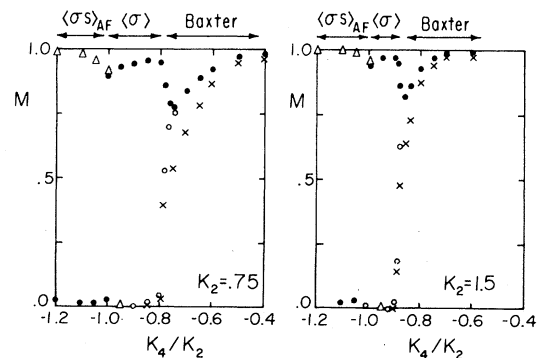


FIG. 8. Plots of different kinds of magnetizations as a function of $x = K_4/K_2$ for $K_2 = 0.75$ and 1.5 for a $10 \times 10 \times 10$ lattice. The triangles represent $|\langle \sigma S \rangle_{AF}|$ the closed and open circles the larger and the smaller of $\langle \sigma \rangle$ and $\langle S \rangle$ (called M_1 and M_2 in the text) and the cross represents $\langle \sigma S \rangle$. When a symbol is not shown, the corresponding magnetization is zero.

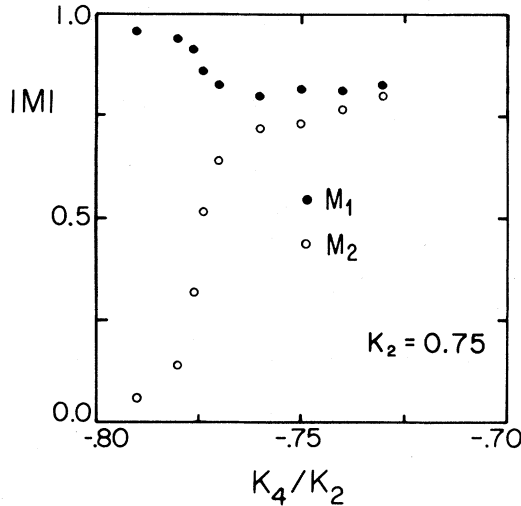


FIG. 9. Plot of M_1 and M_2 as a function of x for $K_2 = 0.75$ for a $14 \times 14 \times 14$ lattice.

into a "Baxter" phase in which $|\bar{\sigma}| \approx |\bar{S}|$ is of order unity. However for $-0.75 \geq x \geq -0.78$, an unexpected behavior occurs. The system seems to have both $\bar{\sigma}$ and \bar{S} different from zero but $\bar{\sigma} \neq \bar{S}$. The system seems to have two fixed values of the magnitudes of the order parameter, M_1 and M_2 , with $M_1 > M_2$. For a while $|\bar{\sigma}| = M_1$ and $|\bar{S}| = M_2$. Then after a time the roles will interchange and $|\bar{\sigma}| = M_2$ and $|\bar{S}| = M_1$. Figure 9 shows a plot of apparent M_1 and M_2 values. If there is really a range in which $M_1 > M_2 > 0$, this is a new phase not seen in mean-field theory. However, the range for which this occurs is very narrow, and even though the result does not seem to change with changes in lattice size (from $10 \times 10 \times 10$ to $14 \times 14 \times 14$), it may nonetheless be a finite-lattice effect.

APPENDIX A

In this Appendix, we sketch some details of the importance-sampling Monte Carlo technique,²⁰ as applied to the Ashkin-Teller model in three dimensions. Most of our data were taken on a $10 \times 10 \times 10$ lattice with periodic boundary conditions using a code written in FORTRAN. The time needed for each spin-flip trial was about 175 μ sec (including the time for computing averages) on a CDC 6600.

Typically, starting from an equilibrium configuration at a nearby point in (K_2, K_4) space, the system was allowed to equilibrate at the new K_2 and K_4 values by making 100–200 passes through the entire lattice. We tested several different sequences of spin-flip trials. The first consisted in going through the simple cubic lattice and at each site considering first the σ spin and then the S spin as the "reference" spin. In the second, during the first pass through the

lattice, at each lattice site, only the σ spin was considered as the "reference" spin and during the second pass, the S spins were candidates for the spin-flip trial. It was found that the latter method took significantly longer to equilibrate the system than the former starting from an ordered nonequilibrium configuration, so that only the former method was used in actual runs.

For large values of x ($x = K_4/K_2 > 4$), it was found to be advantageous to consider the σ and S spins on the same site simultaneously as candidates for a spin-flip trial. Around the temperature where the σ and S spins became disordered, while the product σS remained ordered, this led to an efficient way of equilibrating the system starting from an ordered state.

The transition temperature was identified as the point of maximum slope in internal energy (and) or the appropriate order parameter as a function of temperature. Due to finite-size effects,²¹ we expect our transition temperatures to be systematically, but only slightly different from the true transition temperature.

A first-order transition is signaled by hysteresis and discontinuous jumps in the internal energy and/or the order parameter. As noted by Landau and Binder,²² first- and second-order transitions may be distinguished by the buildup of the magnetization on quenching the system from a disordered state (corresponding to an equilibrium configuration at very high temperatures) to a temperature just below the transition temperature. Due to the presence of long-lived metastable states, a two-step relaxation process is expected in the case of a first-order transition, whereas a smooth buildup is observed in the case of a continuous transition.

APPENDIX B

The series, whose derivation we describe here, are not included for reasons of space. They can be obtained on request from the authors or from the Physical Review depository.

The quantities calculated for high-temperature expansions were: (i) free energy—11 terms; (ii) susceptibility—10 terms; (iii) polarization susceptibility—10 terms. The quantities calculated for low-temperature expansions were: (i) free energy; (ii) magnetization and susceptibility; (iii) polarization and its susceptibilities. The high-temperature series made use of the skeleton graph list of Fisch²³ and his lattice constants which go up to 10 lines. We added the 11th line graph for the free energy.

The partition function is linearized to be²

$$z = \text{Tr} \prod_{\langle ij \rangle} \exp(-\beta H_{ij}) \\ = \text{Tr} \prod_{ij} W [1 + y(\sigma_i \sigma_j + S_i S_j) + z \sigma_i \sigma_j S_i S_j] ,$$

where

$$W = \cosh^2 K_2 \cosh K_4 + \sinh^2 K_2 \sinh K_4 ,$$

$$y = \tanh K_2 (1 + \tanh K_4) / (1 + \tanh^2 K_2 \tanh K_4) ,$$

$$z = (\tanh^2 K_2 + \tanh K_4) / (1 + \tanh^2 K_2 \tanh K_4) .$$

The result is that

$$f = \ln 4 + d \ln W + \sum a_{n,m} y^n z^m ,$$

$$\frac{1}{2} \chi = \frac{1}{2} + \sum b_{n,m} y^n z^m , \quad \frac{1}{2} \chi_p = \frac{1}{2} + \sum c_{n,m} y^n z^m .$$

Using the primitive series-expansion method described in Domb²⁴ with different bonds for σ , S , and σS one obtained the coefficients from the workings of all possible skeleton graphs with n σ and S bonds and m σS bonds.

Susceptibility graphs have two special vertices with free σ variables; polarization susceptibility graphs have two vertices with free σS variables. The process was computerized and for many dimensionality d a set of three matrices can be produced $a_{n,m}$, $b_{n,m}$, and $c_{n,m}$. The matrices for $d=3$ are included in the Physical Review depository. Others are available on request too.

We chose to analyze these series in two variables by setting the ratio of $x = K_4/K_2$ constant and obtaining a series in the one variable K_2 . Pade analysis using a variant of the Elliott program²⁵ was done on $\partial \ln \chi / \partial \tanh K_2$ and $\partial \ln \chi_p / \partial \tanh K_2$. Poles and residues were estimated in the standard way.

The high-temperature free-energy analysis was done by taking Pade approximants of $F - 3 \ln W$, series part and then adding $\ln 4 + 3 \ln W(x)$ to the result.

The low-temperature series were calculated by an extension of the method of Sykes *et al.*²⁶ We included all graphs containing up to six points together with some of the more connected graphs of seven and eight points. Unlike the Ising case or even the four-

state Potts case, each graph here has a different weight so all lattice constants are needed and not only sums of certain groups. We used Sykes and co-workers Ising series coefficients²⁷ as checks on ours as they are sums of groups of graphs with equal number of lines.

Each graph is evaluated by a small computer program which sums up the various possibilities for overturning σ and S at each vertex. For the cases in which, respectively, σ , S , or both are overturned at a given vertex, the appropriate vertex weights are X^d , X^d , and Z^{2d} . Here, $X = \exp[-4(K_2 + K_4)]$, $Z = \exp(-4K_2)$. Each low-temperature contribution must also be multiplied by an appropriate factor describing the configuration of the nearest-neighbor bond. The four types of bond factors are, respectively, obtained when one (a) overturns σ at both ends of a bond; (b) overturns σ at one end and S at the other; (c) overturns σ at one end and both spins at the other; (d) overturns all four spins in the band. In these four cases, the resulting bond weight is, respectively, X^{-1} , ZX^{-1} , Z^{-1} , Z^{-2} . Finally, each of these overturning possibilities is weighted by a factor which depends upon the number of sites at which only σ is overturned (N_σ), the number of sites at which only S is overturned (N_S), and the number at which both are overturned ($N_{\sigma S}$). The magnetization and polarization, susceptibility are, respectively, multiplied by factors of $(2N_\sigma + 2N_{\sigma S})$, and $(2N_\sigma + 2N_S)$.

ACKNOWLEDGMENTS

This work was supported in part by the Materials Research Laboratory Program of the National Science Foundation at the University of Chicago, by NSF Grants No. DMR 77-12637 and No. DMR 77-07723. This work was also supported in part by the Materials Research Laboratory Program of the National Science Foundation at Purdue University by Grant No. DMR 77-23798.

¹J. Ashkin and E. Teller, Phys. Rev. **64**, 178 (1943).

²R. V. Ditzian, Phys. Lett. A **38**, 451 (1972); J. Phys. C **5**, L250 (1972).

³A. C. Brown (private communication).

⁴F. J. Wegner, J. Phys. C **5**, L131 (1972).

⁵C. Fan and F. Y. Wu, Phys. Rev. B **2**, 723 (1970).

⁶R. Baxter, Phys. Rev. Lett. **26**, 832 (1971); Ann. Phys. (N.Y.) **70**, 193 (1972).

⁷H. J. F. Knops, J. Phys. A **8**, 1508 (1975).

⁸M. E. Fisher and R. J. Burford, Phys. Rev. **156**, 583 (1967).

⁹J. C. LeGuillou and J. Zinn-Justin, Phys. Rev. Lett. **39**, 95 (1977). Exponents quoted here are used throughout this work.

¹⁰K. G. Wilson and M. E. Fisher, Phys. Rev. Lett. **28**, 240 (1972).

¹¹A. Aharony, in *Phase Transitions and Critical Phenomena*, edited by C. Domb and M. S. Green (Academic, New York, 1976), Vol. 6; see also, J. Rudnick, Phys. Rev. B **18**, 1406 (1978).

¹²J. R. Banavar, D. Jasnow, and D. P. Landau, Phys. Rev. B **20**, 3820 (1979).

¹³The utility of several complementary methods in the analysis of complex phase diagrams has recently been stressed by S. J. Knak-Jensen, O. G. Mouritsen, E. K. Hansen, and P. Bak, Phys. Rev. B **19**, 5886 (1979).

¹⁴L. P. Kadanoff and F. J. Wegner, Phys. Rev. B **4**, 3989 (1971).

- ¹⁵R. Brout, *Phase Transitions* (Benjamin, New York, 1965).
- ¹⁶L. P. Kadanoff, W. Gotzee, R. Hecht, E. A. S. Lewis, V. V. Palciauskas, M. Rayl, and J. Swift, *Rev. Mod. Phys.* 39, 395 (1967); A. B. Harris, Lectures at Banff (1979) (unpublished).
- ¹⁷R. V. Ditzian and L. P. Kadanoff, *J. Phys. A* 12, 1229 (1979).
- ¹⁸D. M. Saul, M. Wortis, and D. Stauffer, *Phys. Rev. B* 9, 4964 (1974).
- ¹⁹It is instructive to compare our results with those of D. Jasnow and M. Wortis, *Phys. Rev.* 176, 739 (1968) and M. E. Fisher and D. R. Nelson, *Phys. Rev. Lett.* 32, 1350 (1974).
- ²⁰Our Monte Carlo code was patterned on that described by D. P. Landau, *Phys. Rev. B* 13, 2997 (1976).
- ²¹M. E. Fisher, in *Proceedings of the International Summer School, Varenna, Italy, 1970*, edited by M. S. Green (Academic, New York, 1972).
- ²²D. P. Landau and K. Binder, *Phys. Rev. B* 17, 2328 (1978).
- ²³R. Fisch, Ph.D. thesis (University of Pennsylvania) (unpublished).
- ²⁴C. Domb, in *Phase Transitions and Critical Phenomena*, edited by C. Domb and M. S. Green (Academic, New York, 1974), Vol. 3, pp. 1–42.
- ²⁵C. Elliott (private communication).
- ²⁶M. F. Sykes, J. W. Essam, and D. S. Gaunt, *J. Math. Phys.* 6, 283 (1965).
- ²⁷C. Domb, in *Phase Transitions and Critical Phenomena*, edited by C. Domb and M. S. Green (Academic, New York, 1974), Vol. 3, p. 414.